

On Impact of Topology and Cost Function on LSE Position Determination in Wireless Networks

Vedran Dizdarević and Klaus Witrisal
 {v.dizdarevic,witrisal}@TUGraz.at

Signal Processing and Speech Communication Laboratory
 Graz University of Technology

Abstract - In this work, effects of the anchor nodes geometry on the positioning error are evaluated for a least squares estimation (LSE) of the linearized multilateration problem. It is shown that for different node topologies, the choice of the cost function has a significant impact on the variance and bias of the averaged position error. The importance of knowledge of the range error model is discussed. Monte-Carlo simulations are presented, which verify the results of theoretic discussions. It is shown that an unbiased averaged position error can be obtained in the case when biased and correlated range estimates are present.

1 Introduction

Emerging technologies, such as UWB, have increased the interest in geopositioning applications in traditionally harsh radio environments. Indoor-to-indoor and indoor-to-outdoor transmissions are used to measure distances between wireless devices. A number of such measurements can be combined to determine the unknown position of the mobile device. Such an approach requires a predeployed infrastructure of anchor nodes, which are used as references in the positioning process. In this work a positioning scenario based on multiple time-of-arrival (ToA) estimates, followed by position determination based on spherical multilateration is evaluated.

Anchor geometry and the error model underlying single distance measurements are known to be major factors constraining accuracy in wireless positioning [2],[5]. While some applications will allow for full control over the anchor topology, in others this will not be possible. One such example is positioning of personnel in emergency situations using a temporary reference infrastructure.

Different degrees of knowledge of the range error model allow for different algorithms to calculate the unknown position. Known error statistics allow for the maximum likelihood (ML) solution, which is optimal for the given set of observations and a known error distribution [4]. Exact parameters of range error statistics highly depend on the propagation environment. For this reason this approach is of limited value for generic application scenarios. The LSE solution is a good choice when the error distribution is not known. It is computed such that a given cost function $J(\boldsymbol{\theta})$ is minimized in the unknown position parameter $\boldsymbol{\theta}$. As $J(\boldsymbol{\theta})$ is not a general optimality criterion, its choice will effect the overall positioning accuracy. Further it will be shown that knowledge of the *structure* of the error model can also be used to choose an appropriate cost function $J(\boldsymbol{\theta})$.

Two different position estimation approaches with different cost functions will be presented in Section 2. A description of the simulation environment as well as obtained simulation results follow in Section 3. Effects of the linearization of the problem on the dilution of precision are discussed. This paper is concluded with a brief summary of results and a critical review of their general validity in Section 4.

2 LSE Positioning Algorithms

The two-dimensional multilateration problem resulting from k distance measurements to anchor nodes is formulated in (1), in which $[x_i \ y_i]^T$ is the known position of i -th anchor.

$$\begin{pmatrix} (x_1 - \theta_x)^2 + (y_1 - \theta_y)^2 \\ \vdots \\ (x_k - \theta_x)^2 + (y_k - \theta_y)^2 \end{pmatrix} = \begin{pmatrix} \tilde{\rho}_1^2 \\ \vdots \\ \tilde{\rho}_k^2 \end{pmatrix} \quad (1)$$

The set of equations (1) is nonlinear in the unknown position vector $\boldsymbol{\theta} = [\theta_x \ \theta_y]^T$ and lacks a closed-form solution. $\tilde{\rho}_i$ is an estimated distance to the i -th anchor. Throughout the work, the notation $(\tilde{\cdot})$ is used for values which include uncertainties introduced during the estimation process. A cost function typically associated with this problem minimizes the sum of squared distance differences between the observations $\tilde{\rho}_i$ and the distance to the hypothetical position $\boldsymbol{\theta}$ (2).

$$J_1(\boldsymbol{\theta}) = \sum_{i=1}^k (\tilde{\rho}_i - \sqrt{(x_i - \theta_x)^2 + (y_i - \theta_y)^2})^2 \quad (2)$$

Numerical or iterative methods are required to minimize (2). Alternatively, the problem can be redefined in a way that the cost function is linear in the unknown parameters, which leads to closed-form solutions of the position estimation problem.

2.1 Linearized least squares solution

In [1], a simple procedure is described, which produces a set of equations linear in the unknown position vector $\boldsymbol{\theta}$. Subtracting any of k equations from all $k - 1$ others results in a problem that can be written as a linear estimation problem (3) with a closed form solution (4) [3]. The index of the node which is subtracted will be denoted by r . In this process a new set of references $l \in \{1, \dots, k\} \setminus \{r\}$ is defined. The cardinality of the new set is $\text{card}\{l\} = k - 1$.

$$\mathbf{H}\boldsymbol{\theta} = \mathbf{x} \quad (3)$$

$$\boldsymbol{\theta} = (\mathbf{H}^T \mathbf{H})^{-1} \mathbf{H}^T \mathbf{x} \quad (4)$$

The matrix \mathbf{H} is given as in (5) and the observation vector \mathbf{x} corresponds to (6) [1].

$$\mathbf{H} = -2 \begin{pmatrix} (x_1 - x_r) & (y_1 - y_r) \\ (x_2 - x_r) & (y_2 - y_r) \\ \vdots & \vdots \\ (x_{k-1} - x_r) & (y_{k-1} - y_r) \end{pmatrix} \quad (5)$$

$$\mathbf{x} = \begin{pmatrix} \tilde{\rho}_1^2 - \tilde{\rho}_r^2 - x_1^2 + x_r^2 - y_1^2 + y_r^2 \\ \tilde{\rho}_2^2 - \tilde{\rho}_r^2 - x_2^2 + x_r^2 - y_2^2 + y_r^2 \\ \vdots \\ \tilde{\rho}_{k-1}^2 - \tilde{\rho}_r^2 - x_{k-1}^2 + x_r^2 - y_{k-1}^2 + y_r^2 \end{pmatrix} \quad (6)$$

Note that in the linearization step described above, also the cost function has been redefined. For any linear minimization procedure, the cost function is given as in (7) [3]. The new cost function which is minimized in closed form using (4) is given in (8).

$$J_2(\boldsymbol{\theta}) = \|\mathbf{x} - \mathbf{H}\boldsymbol{\theta}\|^2 \quad (7)$$

$$J_2(\boldsymbol{\theta}) = \sum_{i=1}^{k-1} (\tilde{\rho}_i^2 - \tilde{\rho}_r^2 - x_i^2 + x_r^2 - y_i^2 + y_r^2 + 2(x_i - x_r)\theta_x + 2(y_i - y_r)\theta_y)^2 \quad (8)$$

Note a significant difference between $J_1(\boldsymbol{\theta})$ and $J_2(\boldsymbol{\theta})$. In the latter, two error-inducing terms $\tilde{\rho}_i$ and $\tilde{\rho}_r$ are present. As it will be shown in Sections 3 and 4, building the difference of squares of estimated distances in the cost function is useful for certain anchor topologies as it reduces the effects of the biased range estimates on the calculated position. Correlated range error bias among different anchors is assumed in this work. Concepts behind this assumption and the implication on the results are discussed in Section 4.

2.2 Objective function analysis

In the following the cost function from (8) will be rewritten such that the error-inducing terms are separated from the known anchor positions. This results in (9), with newly introduced variables being defined as in (10) and (11). It will be shown, that $J_2(\boldsymbol{\theta})$ is approximated by the same function regardless of the range error model.

$$\begin{aligned} J_2(\boldsymbol{\theta}) &= \sum_{i=1}^{k-1} (\tilde{L}_i + K_{1,i} + K_{2,i}\theta_x + K_{3,i}\theta_y)^2 \\ &= \sum_{i=1}^{k-1} \tilde{L}_i^2 + 2 \sum_{i=1}^{k-1} \tilde{L}_i M_i(\boldsymbol{\theta}) + \sum_{i=1}^{k-1} M_i^2(\boldsymbol{\theta}) \end{aligned} \quad (9)$$

$$\tilde{L}_i = \tilde{\rho}_i^2 - \tilde{\rho}_r^2 \quad (10)$$

$$\begin{aligned} K_{1,i} &= x_r^2 + y_r^2 - x_i^2 - y_i^2 \\ K_{2,i} &= 2(x_i - x_r) \\ K_{3,i} &= 2(y_i - y_r) \\ M_i(\boldsymbol{\theta}) &= K_{1,i} + K_{2,i}\theta_x + K_{3,i}\theta_y \end{aligned} \quad (11)$$

Considering a specific topology, in which base stations are located on a circle and the mobile unit is in the center, exact distance measurements ($\tilde{\rho}_i = d_i$) would lead to $\tilde{L}_i = L_i = 0$ reducing (9) to $J_2(\boldsymbol{\theta}) = \sum_{i=1}^{k-1} M_i^2(\boldsymbol{\theta})$.

Erroneous distance estimates lead to nonzero first and second order terms of \tilde{L}_i and thus to the global minimizer $\boldsymbol{\theta}$ of (9), which does not correspond with the true mobile unit position \mathbf{p} .

Two different error models are typically used to describe range estimation errors for line-of-sight (LOS) and no-line-of-sight (NLOS) propagation [2]. The induced range error for unobstructed transmissions is statistically described by a zero-mean Gaussian variable ϵ_{los} (12).

$$\epsilon_{los} \sim \mathcal{N}(0, \sigma_{los}^2) \quad (12)$$

Larger range error values are expected for NLOS transmissions [2], as the leading edge of the received signal might be very weak or completely obstructed. The error model for the latter case is given in (13), accounting for a bias in the estimated range.

$$\epsilon_{nlos} \sim \mathcal{N}(\mu_{nlos}, \sigma_{nlos}^2) \quad (13)$$

Exploiting the introduced error models for a given set of distance estimates $\{\tilde{\rho}_{los,i}\}$, equation (10) can be calculated as given in (14). Realizations of ϵ_{los} are denoted as s_{los} . Assuming small σ_{los}^2 , the difference of squared terms in (14) can be neglected.

$$\tilde{L}_{los,i} = (d_i + s_{los,i})^2 - (d_r + s_{los,r})^2 = 2d(s_{los,i} - s_{los,r}) + s_{los,i}^2 - s_{los,r}^2 \approx 2d(s_{los,i} - s_{los,r}) \quad (14)$$

In the NLOS case, equal biases $\mu_{nlos,1} = \mu_{nlos,2} = \dots = \mu_{nlos,k}$ of the range errors are assumed. Such an assumption can be made for a set of base stations which are closely spaced and have the same orientation towards the mobile unit. Alternatively it can be argued that the propagation distance is correlated with the NLOS bias as in [2]. Further assuming $d \gg \mu_{nlos,i}$ (10) is calculated in the NLOS case as given in (15).

$$\begin{aligned} \tilde{L}_{nlos,i} &= (d_i + \mu_{nlos} + s_{nlos,i})^2 - (d_k + \mu_{nlos} + s_{nlos,k})^2 \\ &= 2(d_i + \mu_{nlos})(s_{nlos,i} - s_{nlos,k}) + s_{nlos,i}^2 - s_{nlos,k}^2 \approx 2d(s_{nlos,i} - s_{nlos,k}) \end{aligned} \quad (15)$$

Note that under the given assumptions, equivalent representations of \tilde{L}_i are obtained for the LOS and NLOS propagation. Most notably $\tilde{L}_{nlos,i}$ does not depend on $\mu_{nlos,i}$.

3 LSE Positioning Simulations

3.1 Simulation environment

Topology definition

For simplicity, a set of topologies is investigated in this work, which consists of k base stations equidistantly located on the arc of a circle with a given opening angle. The mobile unit position coincides with the center of the circle, which is in the origin of the cartesian coordinate system. The radius d of the circle corresponds to the transmission distance (Fig. 1).

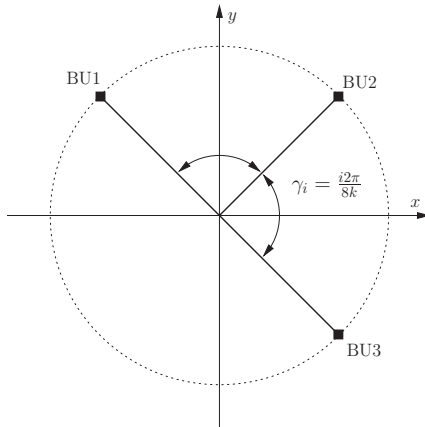
In order to assess the performance of both algorithms, a set of eight topologies is defined, which are labeled with a topology index $i \in \{1, \dots, 8\}$. By defining the opening angle between two neighbouring BUs as (16), it is clear that for $i = 8$, k BUs are distributed over a full circle. For $i < 8$ the BUs are placed on the arc with an overall opening angle of $\Gamma = (k - 1)\gamma_i$ (Fig. 1).

$$\gamma_i = \frac{i2\pi}{8k} \quad (16)$$

Range error model

For simulation purposes a range error model derived from an extensive UWB measurement campaign from 2–6 GHz will be used [2]. The model provides for $\mu_{los,nlos} = f(d)$ and $\sigma_{los,nlos} = g(d)$ as functions of transmission distance. For LOS simulations $\mu_{los} = 0$ and $\sigma_{los}(10m) = 0.383m$. For NLOS simulations all range estimates are biased by $\mu_{nlos}(10m) = 0.44m$ and $\sigma_{nlos} = \sigma_{los}$.

The simulations performed in the next section will reveal that knowledge of the type of error model can be employed to choose the suitable error function.


 Figure 1: Schematic topology definition ($k=3$)

Position error metrics

To assess the performance of both positioning algorithms, a large number ($L = 5000$) of simulations is calculated for all topologies. Two different error metrics are introduced.

In order to analyse the expected bias in the averaged position error equation (17) defines a l^2 -norm of the expectation of the calculated position. θ_l denotes the calculated position for the l^{th} realisation and \mathbf{p} denotes the true position of the mobile unit.

$$\varepsilon_{mean} = \| E\{\theta_l - \mathbf{p}\} \| \approx \left\| \frac{1}{L} \sum_{l=1}^L (\theta_l - \mathbf{p}) \right\| \quad (17)$$

Further a standard deviation is calculated for the magnitude of the positioning errors over all realizations (18). This corresponds to the root mean square (RMS) positioning error.

$$\sigma_\varepsilon = \sqrt{\frac{1}{L} \sum_{l=1}^L (\|\theta_l - \mathbf{p}\| - \|E\{\theta_l - \mathbf{p}\}\|)^2} \quad (18)$$

Finally histograms of the error magnitude are presented and compared for the two algorithms.

3.2 Simulation results

The performance of both described LSE algorithms is assessed in this section through Monte-Carlo simulations. A total of 16 topologies are evaluated for both LOS and NLOS error models. Topologies are divided in two groups, one with a minimally required number of anchors for 2D-positioning $k = 3$ and a strongly overdetermined network with $k = 10$ anchors. It will be assumed that all anchors for a single realisation have either LOS or NLOS. Cases with mixed LOS and NLOS conditions of anchors are not considered.

Equation (2) is minimized by employing a grid search procedure with 1cm accuracy in both x- and y- directions, while (8) is solved by calculating (4).

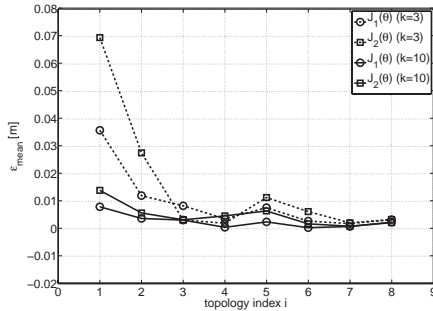
Bias of the averaged solution


Figure 2: Euclidian error distance of the averaged position with LOS range error model

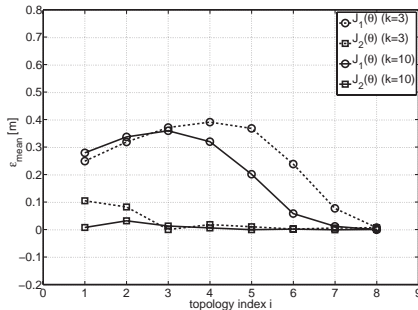


Figure 3: Euclidian error distance of the averaged position with NLOS range error model

Figures 2 and 3 show the bias (Eq.17) in the averaged position for LOS and NLOS ranging. In the LOS case, very small biases are observed for topologies $i \in \{3, \dots, 8\}$. Comparable results are obtained for minimal ($k = 3$) as well as overdetermined ($k = 10$) anchor configurations. Topologies $i \in \{1, 2\}$ show dependence of the performance on the number of anchors k . Compared to $k = 3$, the bias is significantly reduced if $k = 10$. For the same topology index i and the same number of anchors, the minimization of the objective function $J_1(\theta)$ produces a smaller bias in the position error.

For biased range measurements (NLOS) (Fig.3), $J_1(\theta)$ produces a topology-dependent error ε_{mean} . The bias first increases and then decreases with larger γ_i . A significant error of $\varepsilon_{mean} > 20cm$ is calculated for $i \in \{1, \dots, 5\}$ ($k = 3$) and $i \in \{1, \dots, 4\}$ ($k = 10$). The error is less sensitive to topology changes when linearized $J_2(\theta)$ is employed for position calculation. Except for $i \in \{1, 2\}$, the bias is comparable to the one in the LOS case. Overall, $J_2(\theta)$ shows a significantly better performance through a significantly reduced error bias. Also, $J_2(\theta)$ is less sensitive to variations in the number of anchors k .

RMS of the error magnitude

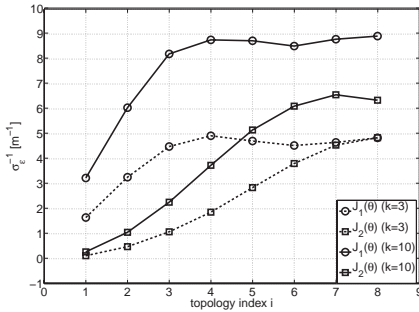


Figure 4: Inverse of the RMS position error for LOS range error model

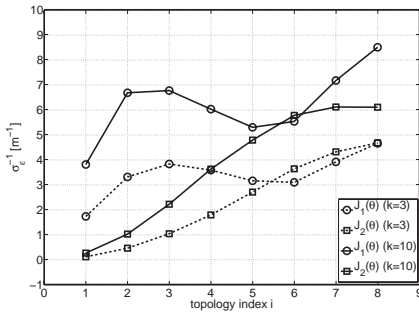


Figure 5: Inverse of the RMS position error for NLOS range error model

In Figures 4 and 5 the inverse of the RMS range error is plotted, thus large values represent good positioning performance with small standard deviation.

Comparing $J_1(\theta)$ and $J_2(\theta)$ for $k = 3$ and the LOS error model (Fig. 4), similar performance is obtained for $i \in \{7, 8\}$. For lower i , $J_1(\theta)$ produces smaller variance. As expected, increasing the number of anchors produces smaller variance for both cost functions. However, for the first topology $i = 1$, only a small improvement is obtained when calculating the position using $J_2(\theta)$.

In the NLOS case (Fig. 5) for $k = 3$, $J_2(\theta)$ has slightly smaller error variance than $J_1(\theta)$ ($i \in \{6, 7, 8\}$). This does not hold if the number of anchors is increased to $k = 10$. For the higher number of anchor nodes, the variance of $J_1(\theta)$ is reduced over all topologies, whereas the variance of $J_2(\theta)$ for $i = 1$ is almost the same.

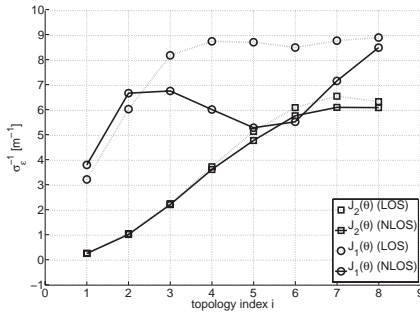


Figure 6: Comparison of the inverse standard deviations for LOS and NLOS error models ($k = 10$)

Comparison LOS/NLOS

As analysed in Section 2.2 the linearized solution exhibits little dependency on the bias in the range estimation (14), (15). In Figure 6, small deviations between LOS and NLOS range estimation are observed.

For $J_1(\theta)$ a significantly higher error variance is present in the NLOS case.

Error magnitude distribution

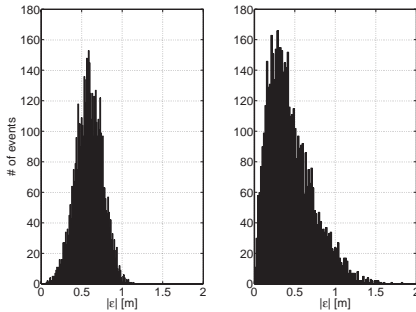


Figure 7: Histograms of the error magnitude for $J_1(\theta)$ (left) and $J_2(\theta)$ (right); $k = 10, i = 4$

For $k = 10$ and $i = 4$ the distribution of the magnitude of the error is plotted in Figure 7. Optimization of $J_1(\theta)$ produces in this case an approximately Gaussian error, whereas this does not hold for the optimization of $J_2(\theta)$.

3.3 Dilution of precision

Dilution of precision is a dimensionless metric which describes how suitable the geometry of a given topology is for position determination. We write the known coordinates of references in vector form (19) and define \mathbf{A} as in (20).

$$\begin{aligned}\mathbf{x} &= [x_1, \dots, x_k]^T \\ \mathbf{y} &= [y_1, \dots, y_k]^T\end{aligned}\quad (19)$$

$$\mathbf{A} = \frac{1}{d}[\mathbf{x} \ \mathbf{y}] \quad (20)$$

Dilution of precision is now calculated as in (21).

$$\mathcal{G}_{j1} = \sqrt{\sum_k \text{diag}(\mathbf{A}^T \mathbf{A})^{-1}} \quad (21)$$

When employing the linearized solution, note that the topology is redefined by subtracting coordinates of the reference base station $\{r\}$ from all other $k-1$ BSs. This results in the change of definition of \mathbf{x} and \mathbf{y} according to equation (22). With $\hat{\mathbf{A}} = \frac{1}{d}[\hat{\mathbf{x}} \ \hat{\mathbf{y}}]$, \mathcal{G}_{j2} is calculated as given in (23).

$$\begin{aligned}\hat{\mathbf{x}} &= [\hat{x}_1, \dots, \hat{x}_{k-1}]^T \\ \hat{\mathbf{y}} &= [\hat{y}_1, \dots, \hat{y}_{k-1}]^T\end{aligned}\quad (22)$$

$$\mathcal{G}_{j2} = \sqrt{\sum_{k-1} \text{diag}(\hat{\mathbf{A}}^T \hat{\mathbf{A}})^{-1}} \quad (23)$$

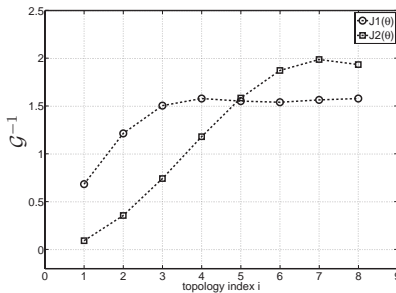


Figure 8: Comparison of \mathcal{G}^{-1} for linearized and non-linearized solutions ($k=3$)

Figure 8 shows the inverse of the dilution of precision \mathcal{G}_{j1}^{-1} and \mathcal{G}_{j2}^{-1} for all investigated topologies and $k = 3$. Local maxima of the function in figure 8 correspond with topologies which are optimal in the sense that the lowest variance in the position error can be expected. For $J_1(\theta)$ two local maxima exist, for $i \in \{4, 8\}$. This corresponds with results obtained in [5].

For $J_2(\theta)$ a different behaviour emerges. The inverse of the dilution is monotonically increasing for $i \in \{1, \dots, 7\}$ and drops slightly for $i = 8$. The global maximum exists at $i = 7$.

4 Conclusion

This work shows that unbiased averaged position estimation can be achieved even in the case when only biased range estimates are available.

By taking note of different cost functions that emerge for different position solutions, a choice can be made, which promises a better accuracy if an assumption on the underlying error model can be made. In this work equal biases in NLOS transmissions are assumed. This correlation assumption will not hold in a general case, in which mixed LOS and NLOS transmissions will occur. Identification of LOS and NLOS transmissions will thus play an important role in selecting a subset of optimal references which are used to determine a mobile's location.

Generally the error variance of single measurements will not be equal either. In this case a weighted LSE solution shall be employed for position determination.

It is shown that for some topologies the advantage of the closed form solution results in higher error deviations.

Acknowledgement

This work has been conducted within the FP6 funded project, EUROPCOM (IST-004154).

References

- [1] M.-G. Di Benedetto and G. Giancola, *Understanding UWB Radio Fundamentals*, 1st ed. Prentice Hall Communications Engineering and Emerging Technologies Series, 2004.
- [2] B. Denis, J. Keignart and N. Daniele, *Impact of NLOS Propagation Upon Ranging Precision in UWB Systems*, IEEE Conference on Ultra Wideband Systems and Technologies, Nov. 2003, pp. 379-383.
- [3] S. M. Kay, *Fundamentals Of Statistical Signal Processing, Estimation Theory*, Prentice Hall PTR, 1993.
- [4] L. Cong and W. Zhuang, *Non-Line-of-Sight Error Mitigation in Mobile Location*, IEEE Conference on Computer Communications, INFOCOM, Vol.1, March 2004, pp. 659-663.
- [5] M.A. Spirito, *On the Accuracy of Cellular Mobile Station Location Estimation*, IEEE Transactions on Vehicular Technology, Vol.50, No.3, May 2001, pp. 674-685.